

# Continuous Infusion of UHMWPE Particles Induces Increased Bone Macrophages and Osteolysis

Pei-Gen Ren DVM, PhD, Afraaz Irani BS,  
Zhinong Huang MD, PhD, Ting Ma MD, MSc,  
Sandip Biswal MD, Stuart B. Goodman MD, PhD

Published online: 2 November 2010  
© The Association of Bone and Joint Surgeons® 2010

## Abstract

**Background** Aseptic loosening and periprosthetic osteolysis resulting from wear debris are major complications of total joint arthroplasty. Monocyte/macrophages are the key cells related to osteolysis at the bone-implant interface of joint arthroplasties. Whether the monocyte/macrophages found at the implant interface in the presence of polyethylene particles are locally or systemically derived is unknown.

**Questions/purposes** We therefore asked (1) whether macrophages associated with polyethylene particle-induced chronic inflammation are recruited locally or systemically and (2) whether the recruited macrophages are associated with enhanced osteolysis locally.

---

One or more of the authors (SBG, SB, TM, P-GR) have received funding from the National Institutes of Health, National Institute of Arthritis, Musculoskeletal and Skin Diseases, Grant #1R01AR055650 in support of this study.

Each author certifies that his or her institution has approved the animal protocol for this investigation and that all investigations were conducted in conformity with ethical principles of research.

This work was performed at the Orthopaedic Research Laboratories and the Stanford Small Animal Imaging Facility at the Clarke Center at Stanford University, Stanford, CA, USA.

---

P.-G. Ren, A. Irani, Z. Huang, T. Ma, S. B. Goodman  
Department of Orthopaedic Surgery, Stanford University,  
Stanford, CA, USA

S. Biswal  
Department of Radiology, Stanford University,  
Stanford, CA, USA

S. B. Goodman (✉)  
Department of Orthopaedic Surgery, Stanford University  
Medical Center Outpatient Center, 450 Broadway Street,  
M/C 6342, Redwood City, CA 94063, USA  
e-mail: goodbone@stanford.edu

**Methods** Noninvasive in vivo imaging techniques (bioluminescence and microCT) were used to investigate initial macrophage migration systemically from a remote injection site to polyethylene wear particles continuously infused into the femoral canal. We used histologic and immunohistologic staining to confirm localization of migrated macrophages to the polyethylene particle-treated femoral canals and monitor cellular markers of bone remodeling.

**Results** The values for bioluminescence were increased for animals receiving UHMWPE particles compared with the group in which the carrier saline was infused. At Day 8, the ratio of bioluminescence (operated femur divided by nonoperated contralateral femur of each animal) for the UHMWPE group was  $13.95 \pm 5.65$ , whereas the ratio for the saline group was  $2.60 \pm 1.14$ . Immunohistologic analysis demonstrated the presence of reporter macrophages in the UHMWPE particle-implanted femora only. MicroCT scans showed the bone mineral density for the group with both UHMWPE particles and macrophage was lower than the control groups.

**Conclusions** Infusion of clinically relevant polyethylene particles, similar to the human scenario, stimulated systemic migration of remotely injected macrophages and local net bone resorption.

## Introduction

Despite improvements in material technology and surgical technique, aseptic loosening and periprosthetic osteolysis resulting from the generation of wear particles are still major long-term complications of total joint arthroplasty (TJA) [1]. Monocyte/macrophages and their derivatives (foreign body giant cells and osteoclasts) are the key cells at the bone-implant interface of joint arthroplasties.

Particulate debris can activate macrophages and other cells and trigger further cell recruitment, phagocytosis, and the release of factors leading to osteolysis [1, 34, 39, 46]. Macrophages can resorb bone directly or differentiate into osteoclasts, the primary bone-resorbing cells, to undermine the prosthetic bed [3, 33]; furthermore, the increased levels of reactive oxygen species produced during phagocytosis of wear debris will impair periprosthetic bone formation as a result of the increased cytotoxicity to osteoprogenitor cells [46]. Numerous *in vivo* and *in vitro* models have been developed to investigate the interactions among macrophages and other cells, wear debris, and osteolysis [1, 3, 8, 12, 16–20, 22, 29, 30, 33, 34, 42]. Instead of pumping particles into the knee and inserting a solid wire into the femoral medullary canal, we modified the rat model of Kim et al. [18, 22] by implanting a hollow titanium rod in the distal part of the femur and pumping particles into the femoral bone marrow cavity directly. In this modified mouse model, polyethylene particles were infused continuously into the femur through an osmotic pump to simulate the clinical scenario more closely [25, 26, 31, 32].

Although we better understand the events underlying periprosthetic inflammation and osteolysis, whether the generation of wear particles stimulates a localized versus a systemic biologic reaction is unknown. Previously, we reported the systemic migration of reporter macrophages introduced from a remote site to the murine femur containing particles of polymethylmethacrylate (PMMA) [36] using noninvasive *in vivo* bioluminescence imaging (BLI) and fluorescence microscopy. In this previous study, the PMMA particles were administered by a single intramedullary injection, which does not simulate the clinical situation in which wear particles are produced continuously. In addition, PMMA particles are generated from bone cement used in TJA; UHMWPE wear debris simulates particles generated from the bearing surface to reach the bone-implant interface [44]. If wear particles of UHMWPE do stimulate systemic migration of macrophages, then potential therapeutic strategies might be initiated to mitigate this response to limit particle-associated osteolysis.

We therefore posed two questions in the present study: first, are the macrophages associated with particle-induced chronic inflammation locally or systemically derived, and second, are the macrophages recruited to the local site associated with enhanced osteolysis?

## Materials and Methods

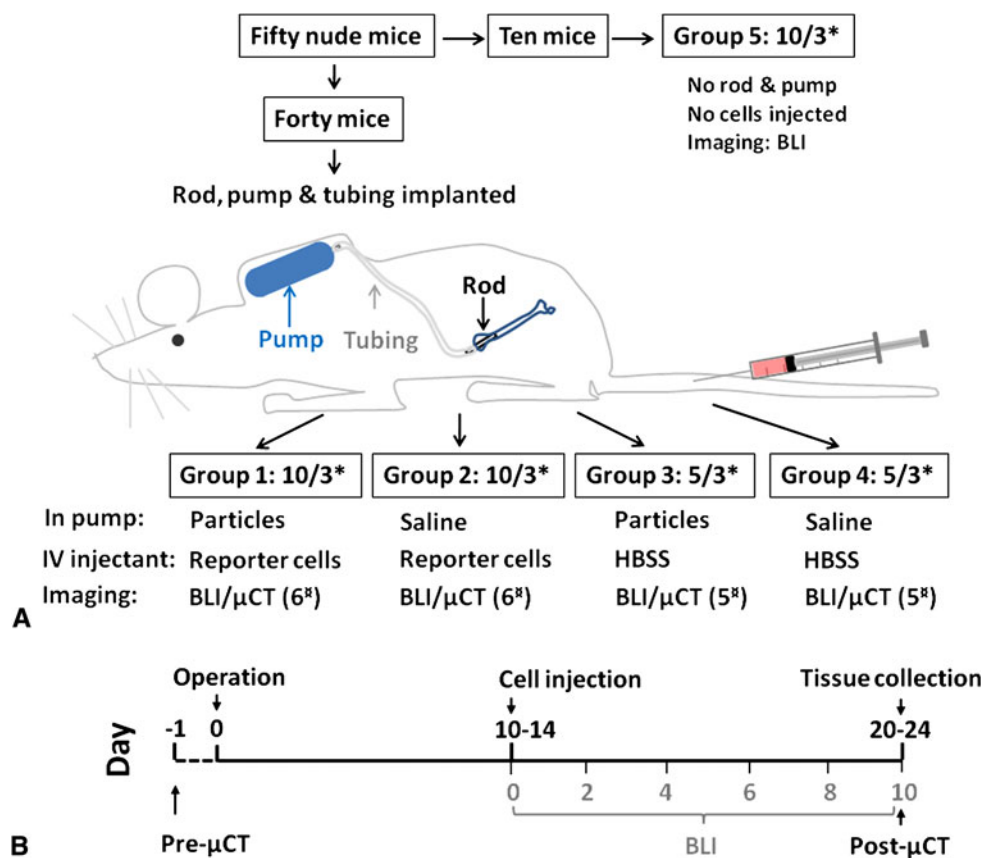
Noninvasive *in vivo* imaging techniques (bioluminescence and microCT) were used to investigate initial macrophage migration systemically from a remote injection site to

polyethylene wear particles continuously infused into the femoral canal. To confirm the localization of the migrated reporter macrophages in the UHMWPE particles infused femora and to detect bone remodeling related cellular markers, histologic and immunohistologic staining were used. In total, 30 successful animals were obtained out of 41 operated nude mice and distributed into four groups: (1) 10 mice had UHMWPE particles in the pump and were injected intravenously with reporter cells; (2) 10 mice had saline in the pump and were injected with reporter cells intravenously; (3) five mice had UHMWPE in the pump and injected intravenously with the carrier solution Hanks' balanced salt solution (HBSS); and (4) five mice had saline in the pump and injected intravenously with HBSS. Another 10 animals received no surgery and therefore served as untreated controls (Fig. 1).

We obtained 12-week-old male immunodeficient nude mice from Charles River Laboratory Inc (Wilmington, MA) and they were maintained in the university's animal facility. Animals were divided into five groups (Groups 1–5) randomly (Fig. 1). The murine macrophage cell line RAW264.7 was transfected with the lentiviral vector to express the bioluminescent optical reporter gene, firefly luciferase (*fluc*), and a fluorescence reporter gene, green fluorescent protein (*gfp*), as previously described [7]. Prior power analysis was based on published data using a similar experimental design [25]. To detect a difference of 1.5 standard deviations from the mean for BLI and bone mineral density (BMD) with a power of 80% ( $\alpha = 0.05$ ,  $\beta = 0.20$ ), nine animals would be needed in each group. We strictly followed Stanford University's guidelines for the care and use of laboratory animals. The murine continuous femoral intramedullary infusion model used in this study was modified from a previously described rat model [22] and validated by successfully pumping UHMWPE and blue polystyrene particles into murine femoral medullary canals [25, 31, 32].

A Model 2006 Alzet osmotic pump was used in the present study and has a mean loading volume of 243  $\mu\text{L}$  and a mean pumping rate of 0.15  $\mu\text{L}/\text{hour}$ . According to the pumping rate and duration of the experiment, approximately 100  $\mu\text{L}$  of the pump contents could be pumped out during 4 weeks. Based on the volume and density of the isolated UHMWPE particles, approximately  $3.0 \times 10^9$  particles were infused into the femoral medullary cavity. Based on previous studies, we presumed the size and the number of particles infused would induce an inflammatory reaction [11, 16, 41]. Conventional (nonhighly crosslinked) UHMWPE particles from mechanical testing simulator studies of metal-on-conventional polyethylene bearings were isolated by ultracentrifugation [5]. The size of the UHMWPE particles was  $1.0 \pm 0.1 \mu\text{m}$  (mean  $\pm$  SE) in length measured by scanning electron microscopy

**Fig. 1A–B** A diagram of the experimental design is shown. (A) Animals were divided into five groups; (B) schedule of experiment. \*The number of animals for histologic analysis; <sup>†</sup>the number of animals for microCT scanning.



(Hitachi S-3400N; Hitachi High-Tech, Tokyo, Japan). Approximately 70% of the particles were submicron and the shape factor of more than 90% of the particles was greater than 2. The particles tested negative for endotoxin using a Limulus Amebocyte Lysate kit (BioWhittaker, Walkersville, MD). The particles were suspended in sterile saline at a concentration of 15 mg/mL (based on the volume and density of the UHMWPE particles isolated, 15 mg/mL equals approximately  $3.1 \times 10^{10}$  particles/mL). Before implantation, we placed particles suspended in saline (15 mg/mL) or saline alone into the pump; particle suspension or saline prefilled and prelinked silicon tubing (6 cm) and a hollow titanium rod (6 mm long, 23 gauge) were connected to the outlet of the pump flow modulator before implantation. Thus, in each osmotic pump, approximately  $7.5 \times 10^9$  particles were loaded. During the 3-week period of implantation, approximately 80  $\mu$ L of the particle suspension could be pumped out theoretically.

Under inhalation anesthesia of 3% to 5% isoflurane in 100% oxygen, animals were operated on a warmed small animal surgery station. Using a sterile technique, a series of needles from 25 gauge to 21 gauge were used to manually drill through the intercondylar notch to access the medullary cavity of the left femur progressively. The osmotic pump was implanted subcutaneously in the interscapular region through a separate incision. The titanium rod was

press-fit into the distal femur, and the connecting tubing was passed through a subcutaneous tunnel. After implant insertion, the quadriceps-patellar complex was repositioned and the medial parapatellar arthrotomy and the dorsal incision for the pump were repaired with sutures and bio-compatible glue. Buprenorphine (0.1 mg/kg; Ben Venue Laboratories, Bedford, OH) was given subcutaneously immediately after surgery and 4 hours later postoperatively for pain control. We checked the animals each day postoperatively. Only the data from the 30 animals with intact connections from the pump to the implanted rod in the femoral cavity during the whole experimental period were included in the final analysis.

Macrophage injections began 10 to 14 days postoperatively when wound healing was satisfactory. We injected reporter macrophages ( $5 \times 10^5$  cells) suspended in 0.1 mL HBSS (Invitrogen, Carlsbad, CA) intravenously through the lateral tail vein of mice. Luciferase substrate D-luciferin (Biosynth International, Itasca, IL) was administered by intraperitoneal injection (3 mg/mouse). Five minutes after substrate injection, bioluminescence images were taken of the entire mouse using an in vivo imaging system (Caliper LifeSciences, Hopkinton, MA) in the Stanford Small Animal Imaging Facility. We obtained prone and lateral images from each animal at each time point to better determine the origin of photon emission.

Animals were imaged at 2-day intervals postmacrophage injection for 10 days. Bioluminescence images were quantified by drawing uniformly sized rectangle regions of interest (ROIs, 0.5 cm × 1.5 cm) over the implanted and contralateral thighs. The data were collected and expressed as photon/second/cm<sup>2</sup>/steradian (p/s/cm<sup>2</sup>/sr). The ratios of BLI (infused versus the contralateral nonoperated limb) for each group were calculated.

We presumed the systemic migration of macrophages to the femur resulting from both UHMWPE particle infusion and remote macrophage injection would increase osteolysis locally in the femur. A previous *in vitro* study showed resorption pits on bone slices incubated with inflammatory cells exposed to particles for 4 days [3]. We performed pre- and postexperimental microCT scans *in vivo* to detect changes in BMD. Before the original surgical procedure while under inhalational anesthesia, animals were scanned using an eXplore RS microCT scanner (GE Medical Systems, Raleigh, NC) with 49- $\mu$ m resolution. To minimize motion artifact, the femora and body were fixed by tape during scanning. After all the BLI studies were completed, animals were euthanized with CO<sub>2</sub> and the implanted titanium rods were removed from the limbs and then microCT scanning was performed again. The image acquisition and reconstruction were completed using eXplore Evolver and eXplore Reconstruction interface software (GE Medical Systems), respectively. The thresholded bone mineral density (TBMD) was quantified based on Hounsfield unit (HU) calibration by using GEMS MicroView software (GE Medical Systems). The TBMD was normalized by subtracting the pretreatment values from postexperimental values of each animal. BMD was analyzed in GEMS MicroView (threshold: 1700 HU) with a phantom calibration for each scan and recorded in milligrams per milliliter of hydroxyapatite. Within the distal part of the femur, a three-dimensional ROI (4 mm × 4 mm × 3 mm) was created, which contained only the diaphysis proceeding proximally beginning 3 mm from the end of the femoral condyles along the femur. For Groups 1 and 2, six animals were randomly selected for microCT scanning and analysis; five mice in Groups 3 and 4 were also scanned. The data from these animals were analyzed blindly.

After completion of the imaging experiments, we collected all femora from the experimental and control groups. Femora from three animals in both the UHMWPE particle and saline groups were randomly chosen for histologic study. Frozen sections were collected from the distal to the middle portion of each femur and used for immunostaining. We used rabbit anti-GFP monoclonal antibody (Chemicon International, Temecula, CA) to detect exogenous macrophages tagged with green fluorescent protein (GFP). Rat antimouse MOMA-2 (AbD Serotec, Raleigh, NC) was used

to detect total macrophages (both injected and noninjected). Mouse antihuman vitronectin receptor  $\alpha$ V $\beta$ 3 antibody (Chemicon International) and anti-osteocalcin antibody (LifeSpan Biosciences, Seattle, WA) were used to identify osteoclasts and osteoblasts, respectively. The secondary antibody used was goat antimouse/rabbit/rat IgG conjugated with Alexa Fluor 488/594 (Invitrogen, Carlsbad, CA). Briefly, phosphate-buffered saline (PBS) buffered paraaldehyde solution (4%)-fixed frozen sections (6  $\mu$ m thick) were blocked by Image-iT™ FX Signal Enhance (Invitrogen) for 30 minutes followed by modified Hank's solution with 10% normal donkey serum for 1 hour at room temperature. Primary antibodies were incubated with sections at 4°C overnight; then the sections were incubated with secondary antibodies for 1 hour at room temperature. ProLong® Gold Antifade Reagent with DAPI (Invitrogen) was used for mounting. We performed washing with PBS between steps. After mounting, images were taken using Nuance multispectral imaging systems (Cri, Woburn, MA). Background autofluorescence was erased by examining the light spectra for specific fluorophores. For each randomly selected sample, we imaged six to eight sections by using the same setting of the program to reduce or erase the autofluorescence.

Hematoxylin and eosin (H&E) staining (Sigma, Steinheim, Germany) was performed to show the general morphology of the femoral section collected as mentioned previously. A leukocyte acid phosphatase kit (Sigma) was used to stain tartrate-resistant acid phosphatase (TRAP) for identification of osteoclasts.

The ratio of the bioluminescence of operated divided by the nonoperated femora within the ROI and TBMD of the microCT analysis of the femora was analyzed by the nonparametric Kruskal-Wallis and Mann-Whitney U tests (two-tailed) between groups (statistiXL, Broadway-Nedlands, Australia).

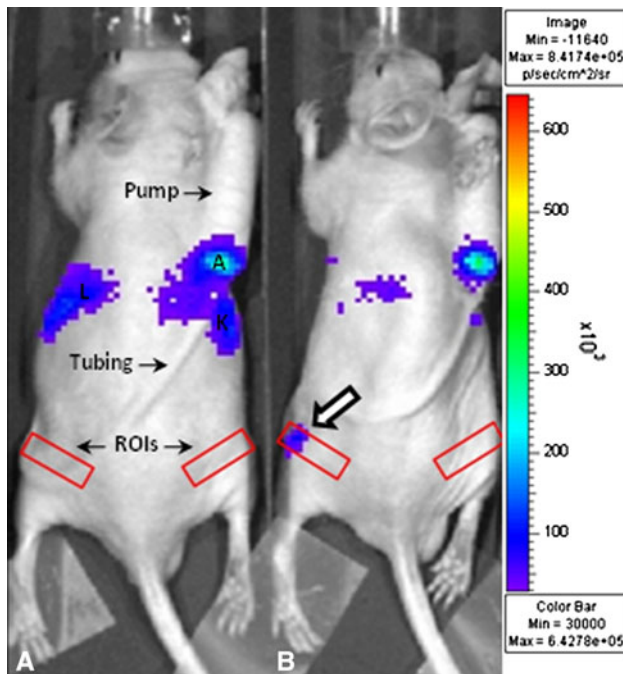
## Results

We confirmed the systemic migration of reporter macrophages by using BLI and immunohistologic staining. Starting from Day 4 postmacrophage injection, higher bioluminescent signal was detected from UHMWPE particle infused femora in Group 1 compared with the other groups (Fig. 2). At Day 8, the ratio for Group 1 was  $13.95 \pm 5.65$ , whereas for Group 2, it was  $2.60 \pm 1.14$ . This value for the bioluminescence in Group 1 was higher ( $p = 0.009$ ) than the Group 2 (Fig. 3). The other three control groups that had no reporter cell injection all had the ratios close to 1.0 from Day 0 to Day 10. H&E-stained sections and immunostaining confirmed localization of the migrated macrophages in the femoral canals treated with

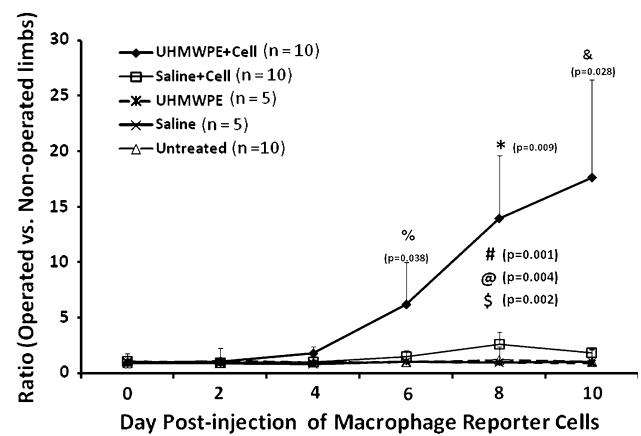
UHMWPE particles (Fig. 4A). TRAP staining indicated the osteoclast-like cells were present in sections from the UHMWPE particle-infused femora of Group 1 (Fig. 4B) but were not found in other groups. The general monocyte/macrophage antigen MOMA-2 and GFP of the reporter macrophages were detected in the femoral canals of UHMWPE particle-infused femora (Figs. 5, 6). Staining

with GFP indicated the macrophages were the injected reporter macrophages (Fig. 5). In contrast, few reporter macrophages were found in femoral sections of Group 2. We observed colocalization of the monocyte/macrophage marker and osteoclast-like cell marker, which indicated the differentiation of macrophages into bone resorbing cells (Fig. 6). In addition, immunofluorescent staining for osteocalcin showed marked fluorescent signals along the trabecular bone, indicating ongoing active bone formation despite heightened macrophage migration to the wear particles (Fig. 7). In contrast, in control groups, few immunofluorescence signals for  $\alpha$ V $\beta$ 3 or osteocalcin were detected.

MicroCT analysis demonstrated a decrease of BMD of femora in Group 1. TBMD increased ( $p < 0.001$ ) in all femora of all the groups after 20 to 24 days regardless of the experimental conditions and operations (Fig. 8A).

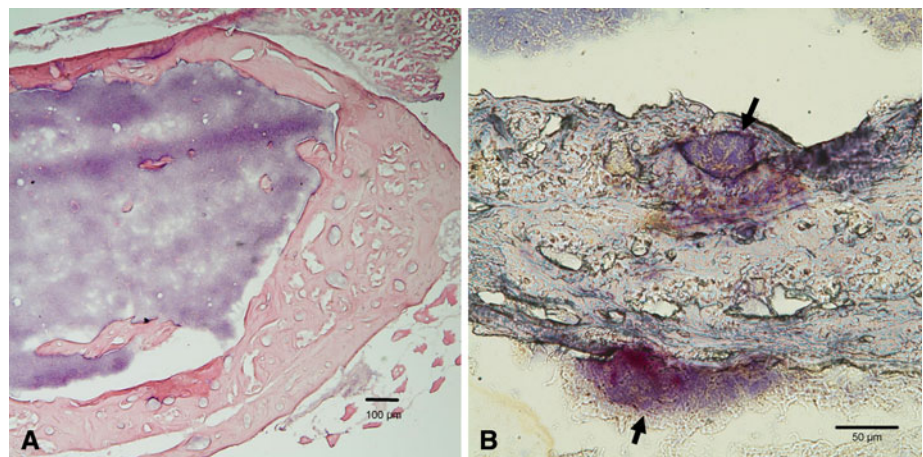


**Fig. 2A–B** A characteristic image of noninvasive in vivo bioluminescence of nude mice with implanted pump systems is shown (Day 6 postmacrophage injection). (A) Shows saline only in the pump; (B) shows UHMWPE particles in the pump. A = autoluminescence signal from the pump; L & K = signal from liver and kidney, respectively. The big arrow indicates the bioluminescence from the femur with infused UHMWPE particles. Signal is measured in p/sec/cm<sup>2</sup>/sr.



**Fig. 3** Curves comparing the ratio of bioluminescence signal from operated femora divided by the signal from corresponding nonoperated contralateral femora from Day 0 to 10 postmacrophage injection. The values are mean  $\pm$  SE. The ratio bioluminescence of Group 1 increased greatly compared with all the control groups. \*Group 1 versus 2; #Group 1 versus 5; @, & Group 1 versus 3; \$, % Group 3 versus 4.

**Fig. 4A–B** Hematoxylin and eosin staining demonstrates the characteristic femoral tissue cross-section (A) and tartrate-resistant acid phosphatase (TRAP) staining shows osteoclast-like cells in frozen sections from Group 1 (B). The arrows in pattern B indicated the TRAP-positive staining osteoclast-like cells (Stain, hematoxylin and eosin; original magnification,  $\times 10$ ; TRAP, original magnification,  $\times 20$ ).



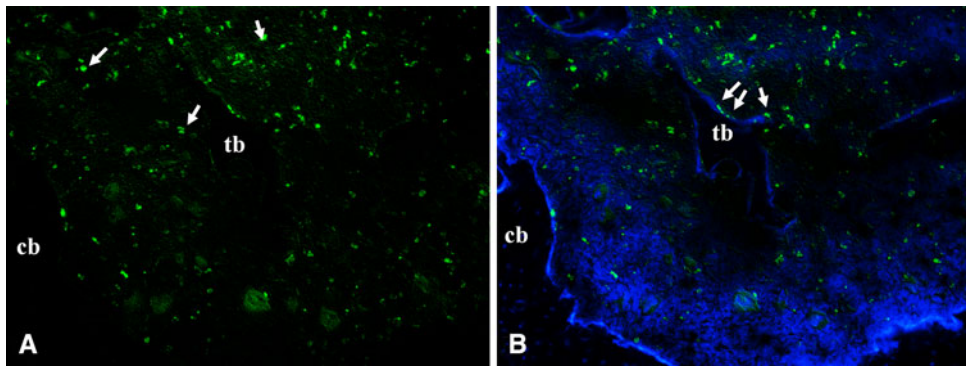
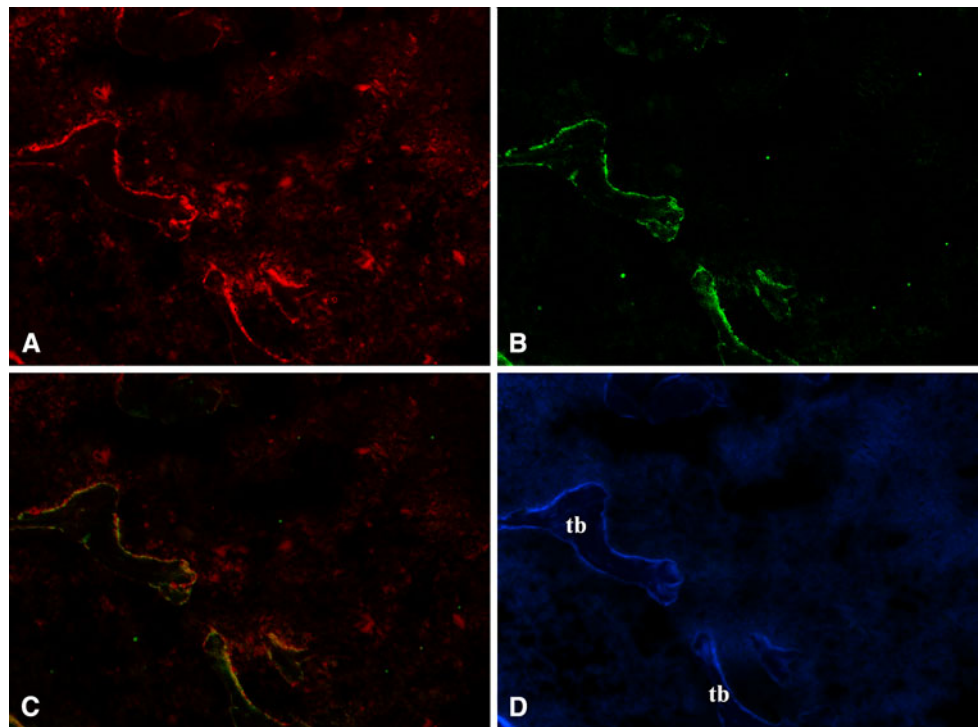


**Fig. 5A–B** Samples from Group 1 were stained with the reporter cell marker green fluorescent protein (GFP). (A) Image taken under FITC filter demonstrating the trafficked macrophages containing GFP (green). (B) Overlay of images A and image taken under DAPI filter

(showing total cell number and bone). Arrows in A and B show the GFP staining signals. “cb” and “tb” refer to cortical bone and trabecular bone, respectively (Stain, immunofluorescence, original magnification,  $\times 20$ ).

**Fig. 6A–D** Samples from Group 1 were double-stained with macrophage marker MOMA-2 and osteoclast-like cell marker  $\alpha V\beta 3$ . (A) Image taken under TRITC filter showing MOMA-2 staining macrophages (red). (B) Image taken under FITC filter showing the osteoclast-like cell marker  $\alpha V\beta 3$  (green). (C) Overlay of A and B using Photoshop. Note the high degree of colocalization of the markers, indicating the macrophages differentiated to osteoclast-like cells. (D) Image taken under DAPI filter. “tb” refers to trabecular bone (Stain, immunofluorescence, original magnification,  $\times 20$ ).



After normalization of the TBMD, the Kruskal-Wallis test indicated differences among the groups ( $p < 0.0001$ ) (Fig. 8B). The combination of UHMWPE and reporter cell infusion was associated with the lowest level of TBMD ( $p$  values were 0.026, 0.017, and 0.017) when compared with Groups 2 to 4 (Fig. 8B). The nonoperated femora of animals in Group 1 also had lower levels of TBMD ( $p = 0.019$ ) when compared with Group 4 (Fig. 8B). The normalized TBMD of nonoperated femora from Group 3 compared with Group 4 also demonstrated a decrease ( $p = 0.016$ ). Among the three control groups, we observed no differences in TBMD in the operated femora.

## Discussion

Aseptic loosening and periprosthetic osteolysis resulting from the generation of particulate wear debris are still major long-term complications of TJA [1]. Although there is more information about the events underlying periprosthetic inflammation and osteolysis, whether the wear particles stimulate a localized versus a systemic biologic reaction is unknown. We tried to answer two questions regarding particle induced osteolysis in this study: (1) whether the macrophages associated with particle-induced chronic inflammation are locally or systemically

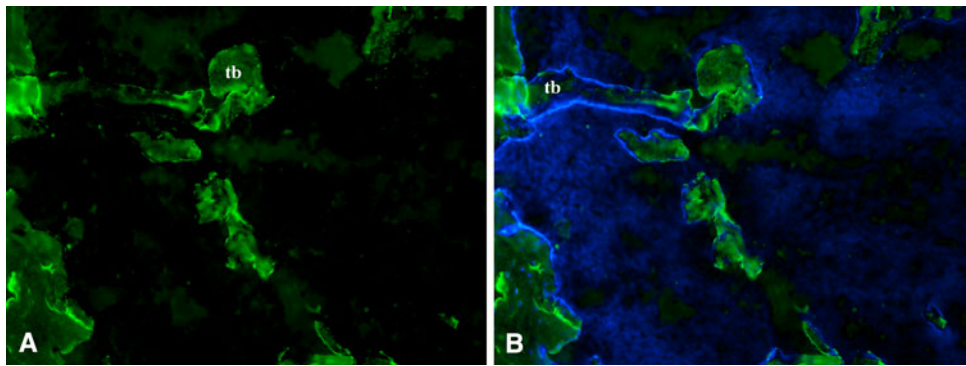
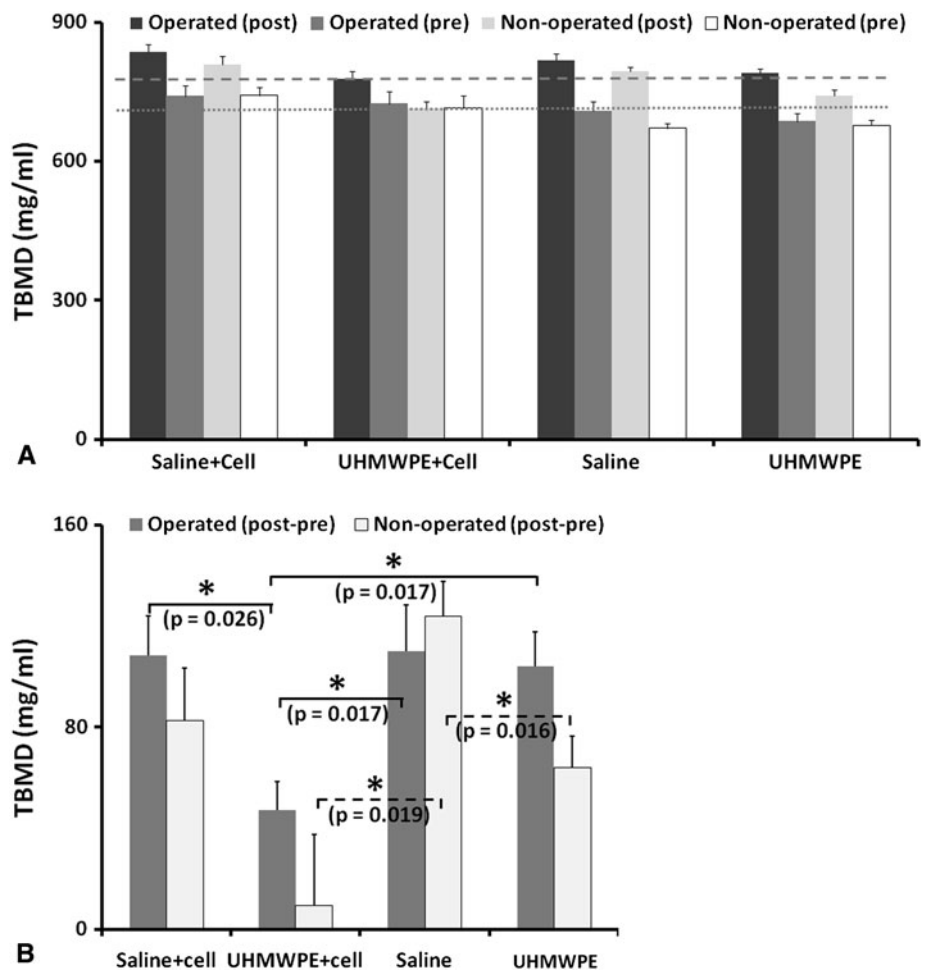


**Fig. 7A–B** Samples from Group 1 were stained with the osteoblast marker osteocalcin. (A) Image taken under FITC filter showing osteocalcin (green) immunostain-positive signals. (B) Overlay of A and image taken under DAPI filter showing the bone and osteocalcin

expressing osteoblasts. Note that the osteocalcin marker localizes primarily to the bone surface. tb refers to trabecular bone (Stain, immunofluorescence, original magnification,  $\times 20$ ).

**Fig. 8A–B** Histogram of the analysis of in vivo microCT scan data. (A) TBMD of pre- and post-microCT scanning of both femora of each mouse in the four groups. Dotted line shows the mean level of prescan TBMD; dashed line shows the TBMD level postscan of Group 1. (B) Normalized TBMD (post minus pre) of both left and right femora of four groups. The TBMD change of operated femora of Group 1 was lower than the other three corresponding control groups. TBMDs of nonoperated femora of Groups 1 and 3 were lower than that of Group 4 (labeled with dashed bar and asterisk). Pre = pre-experimental microCT scan; post = postexperimental microCT scan; post-pre = normalized by postscan value minus prescan value for TBMD. TBMD = total bone mineral density.



derived; and (2) whether the macrophages recruited were associated with enhanced osteolysis locally.

There are some limitations to this study. First, although this mouse model simulates continuous particle production seen clinically, it is a short-term model with an implant that

is load-bearing but not weightbearing. Second, the reporter cells used for tracking of cell migration are an immortal cell line. Consequently, the cells proliferate after their final localization, which could increase the bioluminescent signal. Thus, the bioluminescent signal acquired is a

combination of cell migration and proliferation. Since we cannot distinguish between migration and proliferation in this model, we do not know the relative contribution of either to the final number of macrophages present. Thus it is possible that increased migration as well as proliferation play a role in the response to UHMWPE. Third, the use of a cell line reduced the total observation time as a result of the final onset of cachexia in some of the animals in this experiment after approximately 2 to 3 weeks. By using fewer cells for injection, we could still obtain data for up to 10 days before animals were euthanized.

Macrophages play an important role in wear particle-induced periprosthetic osteolysis [2, 3, 14]. In vivo and in vitro studies have explored the relationship of macrophages and different types of wear particles that are found in periprosthetic tissues [11, 16, 37, 38, 41]; however, only recently [36] has there been direct evidence that some of the macrophages associated with particles in vivo have migrated from a distant site. In the present study, we examined the systemic migration of macrophages in a mouse model with and without intramedullary infusion of UHMWPE particles. By using noninvasive in vivo bioluminescence imaging techniques, we observed real-time cell migration of remotely infused macrophages in the presence of an ongoing particle load using a small animal model. This information increases our understanding of the pathophysiological mechanisms of the chronic inflammatory and foreign body reaction to wear debris from orthopaedic implants and periprosthetic osteolysis [6, 36]. Similar to one-time PMMA particle injection [36], continuously infused UHMWPE particles induced considerable migration of remotely injected macrophages. The distribution pattern of the macrophages in animals was coincident with that reported by others [13, 24]. To further demonstrate the migration of reporter macrophages, we also used immunohistologic techniques to detect migrated reporter cells in the femoral bone marrow. By using an advanced fluorescence imaging system, we reduced/erased autofluorescence originating from collagen [27, 28], which previously was a major obstacle for fluorescence techniques in bone-related studies.

We also detected an increased level of bone remodeling and osteolysis locally in the particle-treated femora similar to the processes of bone remodeling in TJA [1, 4, 45]. Enhanced bone remodeling stimulated by the infusion of UHMWPE particles is in agreement with the report of Kadoya et al. [19] who described similar findings in the bone bed of revised hip arthroplasties. We also demonstrated macrophage to osteoclast-like cell differentiation by double immunostaining of specific cell markers, which was also comprehensively studied by Athanasou and colleagues [3, 35, 40]. Small animal microCT scanning is widely used for evaluating the outcome of bone remodeling. Our data

were consistent with previous studies that UHMWPE particles and other particles types will induce osteolysis [4, 45]. We also observed that bone density was also decreased in the contralateral nonoperated femora in the UHMWPE groups compared with the saline group. As noted previously [36], the systemic effects induced by the UHMWPE particles and activated macrophages stimulated low macrophage migration to the nonoperated contralateral femora, which was confirmed histologically. The changing of TBMD of nonoperated femora might reflect systemic signaling in the body induced by chronic inflammation. The migration of macrophages induced by systemic signaling to the nonoperated limb has also been observed in other inflammatory models and human conditions [9, 10, 21, 23]. The data of TBMD analysis shown here indicate continuous UHMWPE particle infusion may induce osteolysis systemically to some degree as a result of increased numbers of macrophages in the systemic circulation. Analysis of BMD of other bones, for example, the tibia, might give a clearer perspective of this potential effect.

Using the murine continuous femoral infusion model, we observed reporter macrophage migration from the systemic circulation into the medullary cavity of UHMWPE particle-implanted femora during the 2- to 3-week real-time surveillance period. The recruitment of macrophages to the femur also led to localized osteolysis and upregulated markers for bone remodeling. Interference with systemic migration of macrophages may provide a potential therapeutic treatment for the mitigation of osteolysis secondary to polyethylene wear debris. Treatment with small molecules that interfere with cell migration has been shown to have therapeutic potential in diseases such as rheumatoid arthritis [43], lymphoma [15], and other immune diseases [47]. However, biologic modulation of macrophage migration may also interfere with other important, macrophage-associated host defense mechanisms such as infection and tumor surveillance.

**Acknowledgments** We thank Dr Afraaz Irani for performing the bone mineral density analysis of the microCT scans. We thank Dr Gobalakrishnan Sundaresan who supplied the Fluc and GFP expressing RAW264.7 macrophage cell line, Dr Timothy Wright (Hospital for Special Surgery, New York, NY) who supplied the UHMWPE particles, and Stephanie Byun for sectioning of samples used in this study. We also thank Dr Lane Smith, Dr Sam Gambhir, and Dr Chris Contag for their helpful advice.

## References

1. Amstutz HC, Campbell P, Kossovsky N, Clarke IC. Mechanism and clinical significance of wear debris-induced osteolysis. *Clin Orthop Relat Res.* 1992;276:7–18.
2. Archibeck MJ, Jacobs JJ, Roebuck KA, Glant TT. The basic science of periprosthetic osteolysis. *Instr Course Lect.* 2001;50: 185–195.



3. Athanasou NA, Quinn J, Bulstrode CJ. Resorption of bone by inflammatory cells derived from the joint capsule of hip arthroplasties. *J Bone Joint Surg Br.* 1992;74:57–62.
4. Bauer TW. Particles and perimplant bone resorption. *Clin Orthop Relat Res.* 2002;405:138–143.
5. Campbell P, Ma S, Yeom B, McKellop H, Schmalzried TP, Amstutz HC. Isolation of predominantly submicron-sized UHMWPE wear particles from periprosthetic tissues. *J Biomed Mater Res.* 1995;29:127–131.
6. Contag PR, Olomu IN, Stevenson DK, Contag CH. Bioluminescent indicators in living mammals. *Nat Med.* 1998;4:245–247.
7. De A, Lewis XZ, Gambhir SS. Noninvasive imaging of lentiviral-mediated reporter gene expression in living mice. *Mol Ther.* 2003;7:681–691.
8. Dean DD, Schwartz Z, Blanchard CR, Liu Y, Agrawal CM, Lohmann CH, Sylvia VL, Boyan BD. Ultrahigh molecular weight polyethylene particles have direct effects on proliferation, differentiation, and local factor production of MG63 osteoblast-like cells. *J Orthop Res.* 1999;17:9–17.
9. Decaris E, Guingamp C, Chat M, Philippe L, Grillasca JP, Abid A, Minn A, Gillet P, Netter P, Terlain B. Evidence for neurogenic transmission inducing degenerative cartilage damage distant from local inflammation. *Arthritis Rheum.* 1999;42:1951–1960.
10. Donaldson LF, Seckl JR, McQueen DS. A discrete adjuvant-induced monoarthritis in the rat: effects of adjuvant dose. *J Neurosci Methods.* 1993;49:5–10.
11. Doorn PF, Campbell PA, Worrall J, Benya PD, McKellop HA, Amstutz HC. Metal wear particle characterization from metal on metal total hip replacements: transmission electron microscopy study of periprosthetic tissues and isolated particles. *J Biomed Mater Res.* 1998;42:103–111.
12. Endres S, Bartsch I, Sturz S, Kratz M, Wilke A. Polyethylene and cobalt-chromium molybdenum particles elicit a different immune response in vitro. *J Mater Sci Mater Med.* 2008;19:1209–1214.
13. Gao J, Dennis JE, Muzic RF, Lundberg M, Caplan AI. The dynamic in vivo distribution of bone marrow-derived mesenchymal stem cells after infusion. *Cells Tissues Organs.* 2001;169:12–20.
14. Glant TT, Jacobs JJ, Molnar G, Shanbhag AS, Valyon M, Galante JO. Bone resorption activity of particulate-stimulated macrophages. *J Bone Miner Res.* 1993;8:1071–1079.
15. Golay J, Introna M. Chemokines and antagonists in non-Hodgkin's lymphoma. *Expert Opin Ther Targets.* 2008;12:621–635.
16. Green TR, Fisher J, Matthews JB, Stone MH, Ingham E. Effect of size and dose on bone resorption activity of macrophages by in vitro clinically relevant ultra high molecular weight polyethylene particles. *J Biomed Mater Res (Appl Biomater).* 2000;53:490–497.
17. Horowitz SM, Gonzales JB. Effects of polyethylene on macrophages. *J Orthop Res.* 1997;15:50–56.
18. Iwase MK, Kang J, Kobayashi Y, Itoh M, Itoh T. A novel bisphosphonate inhibits inflammatory bone resorption in a rat osteolysis model with continuous infusion of polyethylene particles. *J Orthop Res.* 2002;20:499–505.
19. Kadoya Y, Revell PA, al-Saffar N, Kobayashi A, Scott G, Freeman MA. Bone formation and bone resorption in failed total joint arthroplasties: histomorphometric analysis with histochemical and immunohistochemical technique. *J Orthop Res.* 1996;14:473–482.
20. Kahn AJ, Stewart CC, Teitelbaum SL. Contact-mediated bone resorption by human monocytes in vitro. *Science.* 1978;199:988–990.
21. Kelly S, Dunham JP, Donaldson LF. Sensory nerves have altered function contralateral to a monoarthritis and may contribute to the symmetrical spread of inflammation. *Eur J Neurosci.* 2007;26:935–942.
22. Kim KJ, Kobayashi Y, Itoh T. Osteolysis model with continuous infusion of polyethylene particles. *Clin Orthop Relat Res.* 1998;352:46–52.
23. Kumagai K, Vasanji A, Drazba JA, Butler RS, Muschler GF. Circulating cells with osteogenic potential are physiologically mobilized into the fracture healing site in the parabiotic mice model. *J Orthop Res.* 2008;26:165–175.
24. Kuppen PJ, Marinelli A, Camps JA, Pauwels EK, van de Velde CJ, Fleuren GJ, Eggermont AM. Biodistribution of lymphokine-activated killer (LAK) cells in Wag rats after hepatic-artery or jugular-vein infusion. *Int J Cancer.* 1992;52:266–270.
25. Ma T, Huang Z, Ren PG, McCally R, Lindsey D, Smith RL, Goodman SB. An in vivo murine model of continuous intramedullary infusion of polyethylene particles. *Biomaterials.* 2008;29:3738–3742.
26. Ma T, Ortiz SG, Huang Z, Ren P, Smith RL, Goodman SB. In vivo murine model of continuous intramedullary infusion of particles—a preliminary study. *J Biomed Mater Res B Appl Biomater.* 2009;88:250–253.
27. Mansfield JR, Gossage KW, Hoyt CC, Levenson RM. Auto-fluorescence removal, multiplexing, and automated analysis methods for in-vivo fluorescence imaging. *J Biomed Opt.* 2005;10:41207.
28. Mansfield JR, Hoyt C, Levenson RM. Visualization of microscopy-based spectral imaging data from multi-label tissue sections. *Curr Protoc Mol Biol.* 2008;14:19.
29. Mundy CR, Altman AJ, Gondek MD, Bandelin JG. Direct resorption of bone by human monocytes. *Science.* 1977;196:1109–1111.
30. Orishimo KF, Claus AM, Sychterz CJ, Engh CA. Relationship between polyethylene wear and osteolysis in hips with a second-generation porous-coated cementless cup after seven years of follow-up. *J Bone Joint Surg Am.* 2003;85:1095–1099.
31. Ortiz SG, Ma T, Epstein NJ, Smith RL, Goodman SB. Validation and quantification of an in vitro model of continuous infusion of submicron-sized particles. *J Biomed Mater Res B Appl Biomater.* 2008;84:328–333.
32. Ortiz SG, Ma T, Regula D, Smith RL, Goodman SB. Continuous intramedullary polymer particle infusion using a murine femoral explant model. *J Biomed Mater Res B Appl Biomater.* 2008;87:440–446.
33. Pandey R, Quinn J, Joyner C, Murray DW, Triffitt JT, Athanasou NA. Arthroplasty implant biomaterial particle associated macrophages differentiate into lacunar bone resorbing cells. *Ann Rheum Dis.* 1996;55:388–395.
34. Purdue PE, Koulouvaris P, Potter HG, Nestor BJ, Sculco TP. The cellular and molecular biology of periprosthetic osteolysis. *Clin Orthop Relat Res.* 2007;454:251–261.
35. Quinn J, Joyner C, Triffitt JT, Athanasou NA. Polymethylmethacrylate-induced inflammatory macrophages resorb bone. *J Bone Joint Surg Br.* 1992;74:652–658.
36. Ren PG, Lee SW, Biswal S, Goodman SB. Systemic trafficking of macrophages induced by bone cement particles in nude mice. *Biomaterials.* 2008;29:4760–4765.
37. Ren W, Markel DC, Schwendener R, Ding Y, Wu B, Wooley PH. Macrophage depletion diminishes implant-wear-induced inflammatory osteolysis in a mouse model. *J Biomed Mater Res A.* 2008;85:1043–1051.
38. Ren W, Wu B, Mayton L, Wooley PH. Polyethylene and methyl methacrylate particle-stimulated inflammatory tissue and macrophages up-regulate bone resorption in a murine neonatal calvaria in vitro organ system. *J Orthop Res.* 2002;20:1031–1037.
39. Sabokbar A, Itonaga I, Sun SG, Kudo O, Athanasou NA. Arthroplasty membrane-derived fibroblasts directly induce

- osteoclast formation and osteolysis in aseptic loosening. *J Orthop Res.* 2005;23:511–519.
40. Sabokbar A, Pandey R, Quinn JM, Athanasou NA. Osteoclastic differentiation by mononuclear phagocytes containing biomaterial particles. *Arch Orthop Trauma Surg.* 1998;117:136–140.
  41. Schmalzried TP, Jasty M, Harris TP. Periprosthetic bone loss in total hip arthroplasty. Polyethylene wear debris and the concept of the effective joint space. *J Bone Joint Surg Am.* 1992;74:849–863.
  42. Shanbhag AS, Jacobs JJ, Black J, Galante JO, Glant TT. Macrophage/particle interactions: effect of size, composition and surface area. *J Biomed Mater Res.* 1994;28:81–90.
  43. Suchard SJ, Stetsko DK, Davis PM, Skala S, Potin D, Launay M, Dhar TG, Barrish JC, Susulic V, Shuster DJ, McIntyre KW, McKinnon M, Salter-Cid L. An LFA-1 ( $\alpha$ L $\beta$ 2) small-molecule antagonist reduces inflammation and joint destruction in murine models of arthritis. *J Immunol.* 2010;184:3917–3926.
  44. Urban RM, Jacobs JJ, Tomlinson MJ, Gavrilovic J, Black J, Peoc'h M. Dissemination of wear particles to the liver, spleen, and abdominal lymph nodes of patients with hip or knee replacement. *J Bone Joint Surg Am.* 2000;82:457–476.
  45. von Knoch M, Jewison DE, Sibonga JD, Sprecher C, Morrey BF, Loer F, Berry DJ, Scully SP. The effectiveness of polyethylene versus titanium particles in inducing osteolysis in vivo. *J Orthop Res.* 2004;22:237–243.
  46. Wang ML, Sharkey PF, Tuan RS. Particle bioreactivity and wear-mediated osteolysis. *J Arthroplasty.* 2004;19:1028–1038.
  47. Woodside DG, Vanderslice P. Cell adhesion antagonists: therapeutic potential in asthma and chronic obstructive pulmonary disease. *BioDrugs.* 2008;22:85–100.